Talanta 199 (2019) 507–512

Contents lists available at ScienceDirect

Talanta

journal homepage: www.elsevier.com/locate/talanta

Electrogenerated chemiluminescence aptasensor for lysozyme based on copolymer nanospheres encapsulated black phosphorus quantum dots

Hui Liu, Yu Zhang, YongPing Dong*, XiangFeng Chu

School of Chemistry and Chemical Engineering, Hexian Development Institute of Chemical Industry, Anhui University of Technology, Maanshan 243002, China

ARTICLE INFO

Keywords:
Electrogenerated chemiluminescence
Black phosphorusquantum dots
$Ru(bpy)_3^{2+}$
Aptasensor
Lysozyme

ABSTRACT

Black phosphorus quantum dots (BPQDs) can react with $Ru(bpy)_3^{2+}$ to generate strong anodic electrogenerated chemiluminescence (ECL). However, the instability and the lack of functional groups on BPQDs limit its further application in the fabrication of ECL biosensor. In the present work, uniform BPQDs-styrene-acrylamide (St-AAm) nanospheres (BSAN) are synthesized by encapsulating BPQDs into St-AAm copolymer nanospheres. Sufficient amount of BPQDs can be embedded into nanospheres, and react with $Ru(bpy)_3^{2+}$ to generate strong anodic ECL which is comparable to that of pure BPQDs. Amino group of polymer endows BPQDs the ability to connect with DNA, and can be used to fabricate ECL aptasensor for the sensitive detection of lysozyme. The proposed aptasensor shows high sensitivity, good selectivity and stability for the detection of lysozyme in the range of 0.1–100 pg mL^{-1} with a detection limit of 0.029 pg mL^{-1} (3σ). The proposed method reveals the promising ECL sensing application of BP nanomaterials in the detection of various proteins.

1. Introduction

Electrochemistry is a sensitive and convenient method for the determination of many molecules in biological and environmental analysis. In order to improve the detection sensitivity, various nanomaterials were used to modify traditional solid electrodes [1–8]. In the past few decades, layer-structured two dimensional (2D) nanomaterials, such as graphene and transition-metal dichalcogenides, have attracted immense interest in modifying electrode due to their fascinating chemical and physical characters [9,10]. As a new kind of 2D nanomaterials, black phosphorus (BP) nanosheets have been intensely investigated in field-effect transistors, lithium battery, photocatalysis, and gas sensor in recent years [11–17]. Furthermore, ultra-small few layer BPs, also known as black phosphorus quantum dots (BPQDs), exhibit especial optical and electronic properties owing to quantum confinement and edge effects, which are suitable for novel sensing application [18,19]. However, BP nanomaterials are unstable and tend to be oxidized under the atmosphere condition [20]. As a result, it is quite urgent to develop a simple method to improve the stability of BPs in the air. It was reported that styrene/acrylamide (St-AAm) copolymer nanospheres could be synthesized from styrene and acrylamide by emulsifier-free polymeriation [21]. Pang's group further reported that semiconductor QDs and nano-γ-Fe_2O_3 could be embedded into St-AAm nanospheres to construct functional nanospheres, which can be successfully used to detect DNA, proteins, bacteria, and cancer cells [22–27]. Therefore, it is reasonable to deduce that the encapsulation of BPQDs into St-AAm nanosphere might improve its stability. On the other hand, the functional group of St-AAm copolymer will endow the ability of BPQDs to connect with biomolecule to fabricate various biosensors.

Electrogenerated chemiluminescence (ECL) of $Ru(bpy)_3^{2+}$ might be the most famous ECL system and is widely used in the detection of various samples [28–32]. In order to generate ECL, coreactant is often needed in $Ru(bpy)_3^{2+}$ system, including tripropylamine, oxalate, amino acids, and so on [33–38]. It was found in our previous work that CdTe QDs and BPQDs could also act as coreactant to generate ECL with Ru $(bpy)_3^{2+}$, revealing the new role of QDs in ECL investigation [39,40]. However, the ECL application of polymer capped BPQDs has never been reported.

Lysozyme (Lyz) is a ubiquitous protein which can cleave acetyl groups in the polysaccharide wall of many bacteria. As a result, the content of Lyz in blood is considered as an important clinical index for many diseases including leukemia and meningitis. Up to date, many strategies have been proposed for the sensitive detection of Lyz, including fluorescence, electrochemical, photoelectrochemical, and ECL techniques, and many excited results were obtained [41–44]. Due to the importance of Lyz, it is still needed to develop new strategy for Lyz detection.

* Corresponding author.
E-mail address: dongyp@ahut.edu.cn (Y. Dong).

https://doi.org/10.1016/j.talanta.2019.02.099
Received 13 January 2019; Received in revised form 14 February 2019; Accepted 28 February 2019
Available online 02 March 2019
0039-9140/

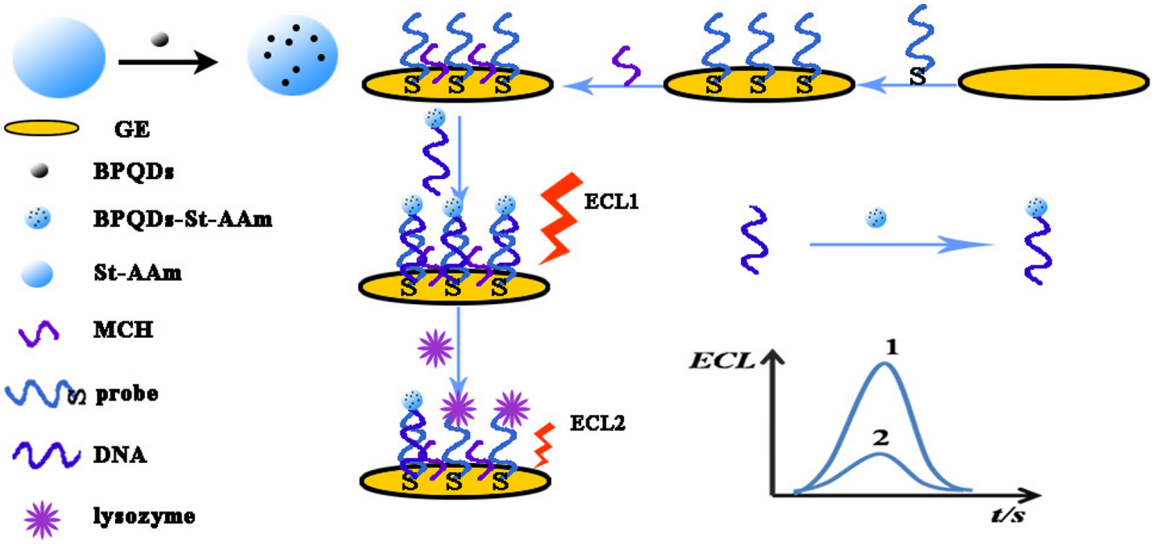

Scheme 1. Schematic representation of the fabrication of ECL biosensor and the detection of lysozyme.

Herein, we prepare BPQDs-St-AAm nanospheres (denoted as BSAN) by embedding BPQDs into poly(styrene/acrylamide) copolymer nanospheres. BSAN can act as coreactant to generate ECL with $Ru(bpy)_3^{2+}$, which is comparable with pure BPQDs. The proposed ECL system can be adopted to fabricate novel aptasensor. As can be from Scheme 1, mercapto group terminated Lyz aptamer was firstly connected onto the gold electrode through S-Au bond as the probe. BSAN was connected with DNA through the amino group on polymer film, and then BSAN/DNA was immobilized onto the electrode through hybridizing with the probe. The connected BSAN could react with $Ru(bpy)_3^{2+}$ to generate strong ECL signal. When the sensor was incubated in Lyz solution, the specific interaction between Lyz and aptamer could release BSAN/DNA from the electrode surface, resulting in the decrease of ECL signal. As a result, a simple and convenient ECL sensing platform was constructed based on BPQDs, $Ru(bpy)_3^{2+}$ and aptamer, which can be used for the sensitive and selective detection of Lyz.

2. Experimental

2.1. Materials and reagents

High-purity black phosphorus crystals were purchased from Nanjing XFNANO Materials Tech. Co., Ltd, China. N-methyl-2pyrrolidone (NMP), lysozyme (from egg white), N-hydroxysuccinimide (NHS), 6-mercapto-1-hexanol (MCH), bovine serum albumin (BSA), 1-ethyl-3-(3-(dimethylamino)propyl) carbodiimide hydrochloride (EDC), tris(2-carboxyethyl)phosphine (TCEP), acrylamide (AAm), styrene (St), thrombin (Thr), horseradish peroxidase (HRP), catalase (Cat), and $Ru(bpy)_3^{2+}$ were obtained from Sigma, USA. 0.1 mol L^{-1} pH 7.4 phosphate buffer solution (PBS) was used to prepare the working solution. All the chemicals were of analytical grade, and were used as received without further purification. Double distilled water was used throughout.

The DNA used in this work was synthesized and purified by Shanghai Sangon Biological Engineering Technology & Service Co., Ltd, China. The sequences of two oligomers employed in the text are given as follows (The italicized part is the complementary strand of oligomers):

The anti-lysozyme aptamer (probe): 3′- **ATC AGG GCT AAA GAG TGC AGA** CCC-$(CH2)_6$-SH-5′.

The complementary DNA: 5′-COOH-TAG TCC CGA TTT CTC ACG TCT-3′

2.2. Preparation of BPQDs

5 mg of BP powder was added into 1 mL of NMP in a mortar and then ground for 20 min. The mixture was transferred to a glass vial containing 3 mL of NMP. After it was sealed carefully, the vial was sonicated in an ice-bath for 8 h at the power of 100 W. The resulting dispersion was centrifuged at 7000 rpm for 20 min and then centrifuged at 10,000 rpm for 20 min. The top 75% of the solution was collected as BPQDs sample. 10 μL of BPQDs suspension was spread onto gold electrode to fabricate BPQDs modified electrode (denoted as BPQDs/GE).

2.3. Synthesis of St-AAm and H_2N-St-AAm nanospheres

150 mL double-distilled water, 5 g AAm, and 0.3 g NaCl were mixed in a four-neck flask equipped with a stirrer and a condenser. After the mixture had been stirred and heated to 70 °C under N_2 atmosphere for at least 15 min, 22 mL St was added and stirred for about 10 min. Potassium persulfate (0.1 g) dissolved in water (20 mL) was introduced while stirring. The polymerization was carried out at 70 °C for 7 h in still N_2 atmosphere. To activate the surface of St-AAm, 20 mL hydrazine was added into 10% St-AAm suspension and heated to 45 °C for 7 h. The produced H_2N-St-AAm was washed with distilled water several times until pH was 7. The product was re-dispersed in water. 10 μL of St-AAm suspension was spread onto gold electrode to fabricate St-AAm nanospheres modified electrode (denoted as St-AAm/GE).

2.4. Synthesis of BPQDs- St-AAm nanospheres

2 mL H_2N-St-AAm suspension and 2 mL BPQDs suspension were mixed and swelled in a chloroform/butanol solvent (5:95 by volume) and then ultrasonicated for 60 min. The mixture was centrifuged for 5 min at 3000 rpm followed by washing three times with butanol to produce the BPQDs-St-AAm nanospheres (BSAN). The product was re-dispersed in 1 mL double-distilled water. 10 μL of BSAN suspension was spread onto gold electrode to fabricate BSAN modified electrode (denoted as BSAN/GE). The synthesized BPQDs and nanospheres were characterized by transmission electron microscopy (TEM) using a JEOL ARM-200F field-emission transmission electron microscope with an acceleration voltage of 200 kV. Fourier transform infrared spectroscopy (FT-IR) was employed to characterize St-AAm nanospheres and BSAN on Nicolet 6700 infrared spectrometer.

2.5. Preparation of BSAN/DNA solution

200 μL of 3 μM complementary DNA was activated with 10 mg mL^{-1} EDC and 5 mg mL^{-1} NHS for 30 min at room temperature. Then, 200 μL of BSAN was added and reacted at 37 °C for 1 h to form BSAN/DNA solution.

2.6. Fabrication of ECL sensor

A gold electrode (2 mm in diameter) was mechanically polished to a mirror with alumina pastes of 0.05 μm, and cleaned thoroughly in an ultrasonic cleaner with alcohol and water sequentially. Then, the electrode was cycled between 0 and 1.50 V (vs. SCE) in 0.50 mol L^{-1} sulfuric acid at a scan rate of 100 mV s^{-1}. This potential cycling was continued until the producible voltammogram for gold oxide formation/reduction was obtained, which meant a clean surface of gold electrode was obtained. The electrode was again rinsed with double-distilled water and cleaned in an ultrasonic bath. 200 μL of 3 μM probe was activated with 5 μL of 10 mM TCEP for 1 h to open disulphide bonds. 10 μL of activated probe was spread on the cleaned gold electrode surface for 1 h at 37 °C. Next, 10 μL of 10 mM MCH was spread on the electrode for 30 min at room temperature to remove the nonspecific probe adsorption. After the electrode was washed with PBS, 10 μL of BSAN/DNA solution was dropped onto the electrode surface to incubate at 37 °C for 1.5 h. The electrode was washed with 10 mM PBS to remove the nonspecific binding BSAN/DNA on the surface. Finally, the resulted electrode was incubated with different concentration of lysozyme for 1 h at 37 °C. After washing with PBS, the modified electrode was used in the ECL measurements. The electrochemical measurements were recorded with CHI 660D electrochemical workstation (CH Instruments Co., China). The ECL measurement was carried out on a model MPI-M electrochemiluminescence analyzer (Xi'An Remax Electronic Science & Technology Co. Ltd., China) at room temperature, and the voltage of the photomultiplier tube (PMT) was set at −800 V during the detection.

3. Results and discussion

3.1. Characterization of BPQDs and BSAN

It was reported that BPQDs can be obtained through exfoliating bulk BP crystals combining grinding and sonication processes. The obtained BPQDs exhibited excellent photothermal and memory performances [45,46]. In our lab, BPQDs are synthesized through the similar method with some necessary revision. The morphology of BPQDs were characterized by transmission electron microscopy (TEM), and high-resolution TEM as shown in Fig. 1. It can be seen from TEM images (Fig. 1a) that BPQDs are uniformly distributed. Fig. 1b reveals that the average size of BPQDs is 8.2 ± 1.1 nm. Fig. 1c and d show the lattice fringes of 0.34 nm and 0.26 nm, which can be ascribed to the (021) and (040) plane of BP crystal, respectively. The thickness of BPQDs ranges from 1.6 to 2.7 nm, corresponding to a stack of 3–5 layers of BP, which was reported in our previous work [40].

In order to facilitate the biosensing application of BPQDs, it is necessary to functionalize BPQDs. Previous work revealed that styrene-acrylamide (St-AAm) copolymer can form uniform nanosphere which can be used to embed various QDs [22–27]. Herein, BPQDs are embedded into St-AAm nanospheres, which is facile for the fabrication of biosensor. The morphologies of St-AAm nanospheres and BPQDs-St-AAm nanospheres (BSAN) were characterized by TEM and HRTEM as shown in Fig. 2. It can be found from Fig. 2a that uniform St-AAm nanospheres are obtained with the average size of ~120 nm. Fig. 2c displays the HRTEM of St-AAm nanospheres and no crystal lattice is obtained (The inset image). When BPQDs was embedded into St-AAm nanospheres, the size of obtained nanospheres is almost the same as that of St-AAm nanospheres (Fig. 2b). The crystal lattice fringes of 0.34 nm and 0.26 nm are found in Fig. 2d, which can be assigned to BP crystal. The TEM results suggest that BPQDs are successfully embedded into polymer nanospheres. The FT-IR spectra were also recorded for polymer nanospheres before and after the doping of BPQDs as shown in Fig. S1. No new peaks are obtained and the positions of the main adsorption peaks are slightly shifted, suggesting that BPQDs are capped by polymer nanospheres but not react with them.

3.2. ECL and electrochemical behaviors of modified electrodes

It was found in our previous work that BPQDs could catalyze the electro-oxidation of $Ru(bpy)_3^{2+}$ [40]. As a result, BPQDs could act as coreactant to generate strong anodic ECL with $Ru(bpy)_3^{2+}$, which revealed new application of BPQDs in ECL field. However, the lack of functional groups on BPQDs make it difficult to immobilize DNA to fabricate ECL biosensor. Herein, styrene-acrylamide copolymer was used to encapsulate BPQDs to form functional nanospheres. The ECL role of the synthesized BSAN was investigated in the presence of $Ru(bpy)_3^{2+}$. As can be seen from Fig. 3a that extremely weak ECL signals are obtained at the bare GE and the St-AAm/GE. Strong anodic $Ru(bpy)_3^{2+}$ ECL can be obtained at the BPQDs/GE because BPQDs can act as the coreactant of $Ru(bpy)_3^{2+}$ just as reported in our previous work [40]. The ECL intensity is slightly decreased at the BSAN/GE. The possible reason is that the capped copolymer film might hamper the charge transfer during ECL process. On the other hand, the nearly similar ECL intensities of the BPQDs/GE and BSAN/GE suggest that large amount of BPQDs can be embedded into polymer nanosphere. Because

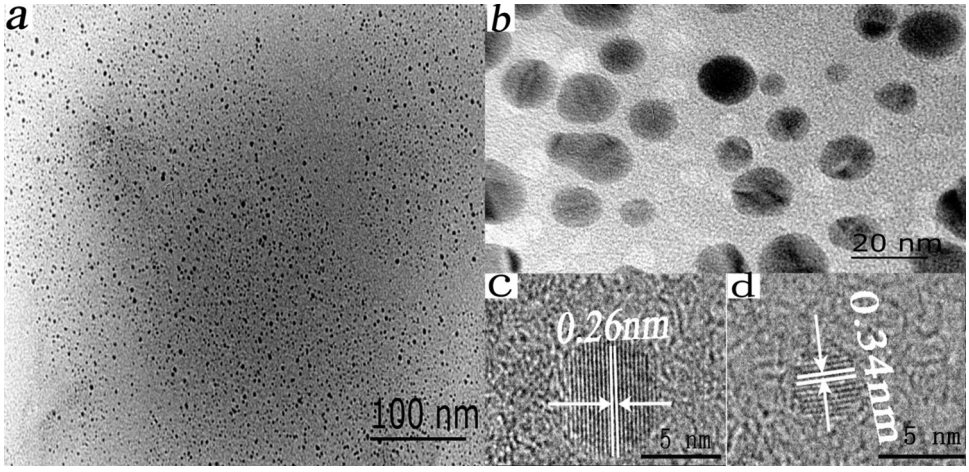

Fig. 1. TEM (a) and HRTEM (b) images of BPQDs. The images of c and d are lattice fringes of (021) an (040) plane of BP crystal.

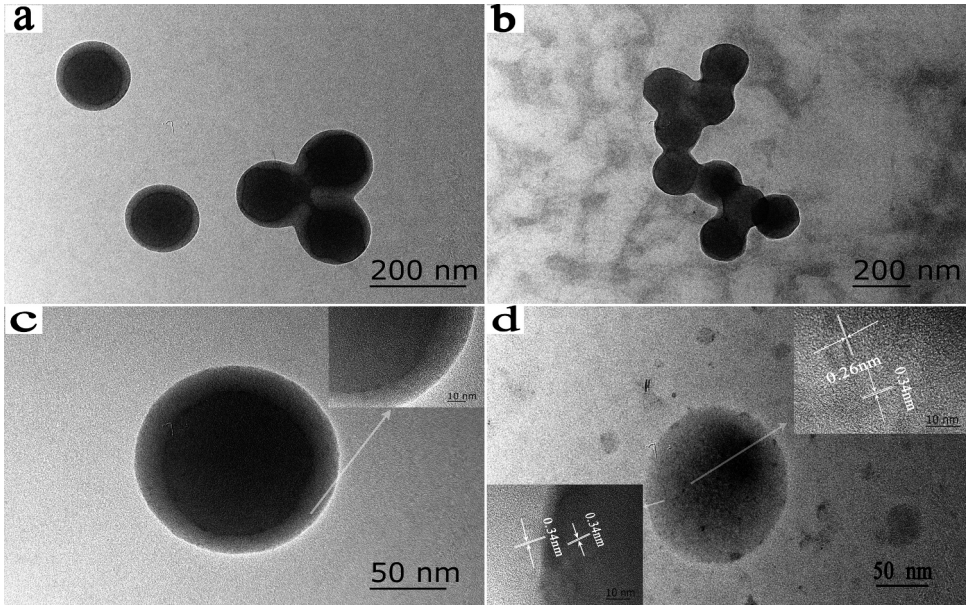

Fig. 2. TEM and HRTEM images of St-AAm nanospheres (a, c) and BSAN (b, d). The insets are the crystal structures of nanospheres.

the existence of functional amino groups from polymer, it is easy for BSAN to connect with different biomolecules to fabricate ECL biosensors.

Cyclic voltammetric technique was used to investigate electrochemical behaviors of $Ru(bpy)_3^{2+}$ on different electrodes as shown in Fig. 3b. When the bare GE was studied in PBS, the oxidation peak at 0.85 V and the reduction peak at 0.4 V can be assigned to the oxidation/reduction processes of gold [47]. In the presence of $Ru(bpy)_3^{2+}$, the oxidation peak of $Ru(bpy)_3^{2+}$ is overlapped with the oxidation of gold, and the peak potential is positively shifted to 0.95 V. Meanwhile, the reduction of $Ru(bpy)_3^{3+}$ is apparently inhibited at the gold electrode. At the BPQDs/GE, the potential of oxidation peak shifts to 0.88 V and the current increases compared to the bare GE, suggesting that BPQDs can catalyze the oxidation of $Ru(bpy)_3^{2+}$. At the St-AAm/GE, the peak potential shifts positively and the current decreases, suggesting that the polymer nanospheres can hamper electron transfer. At the BSAN/GE, the peak potential and the current are almost the same as that of BPQDs/GE, revealing that sufficient amount of BPQDs are embedded into the polymer spheres. The electrochemical and ECL results reveal that polymer capped BPQDs exhibit the similar behaviors as that of pure BPQDs. It was found in the experiment that BSAN is stable in the air, therefore, the synthesized nanospheres will facilitate the ECL application of BP nanomaterials. On the other hand, the existence of the functional amino group on polymer film make it suitable to connect with DNA to fabricate various biosensors.

3.3. Fabrication and characterization of biosensor

Nucleic acid aptamer has high affinity and specificity, and various aptasensors have been proposed based on the specific identification of the aptamers towards their targets. In this work, the BSAN/$Ru(bpy)_3^{2+}$ ECL system was used to fabricate aptasensor for Lyz detection as described in Scheme 1. In order to prove the possibility of the above designs, the ECL signals of each fabrication process were recorded and shown in Fig. 4a. As can be seen, the bare GE and the aptamer modified GE exhibit extremely weak ECL. When BASN/DNA is hybridized with the aptamer, strong ECL emission is obtained due to the reaction between $Ru(bpy)_3^{2+}$ and BPQDs. BASN is released from the electrode surface when Lyz is hybridized with its aptamer, resulting in the decreased ECL intensity. Therefore, the inhibiting effect of Lyz on ECL emission can be used in the determination of Lyz indirectly.

Electrochemical impedance spectroscopy (EIS) was employed to characterize the fabriation process of the aptasensor. It can be found from Fig. 4b that EIS of all electrodes exhibit a semicircle at higher frequency range. The diameter of the semicircle equals the charge transfer resistance (R_{ct}) and can be used to reflect the restricted

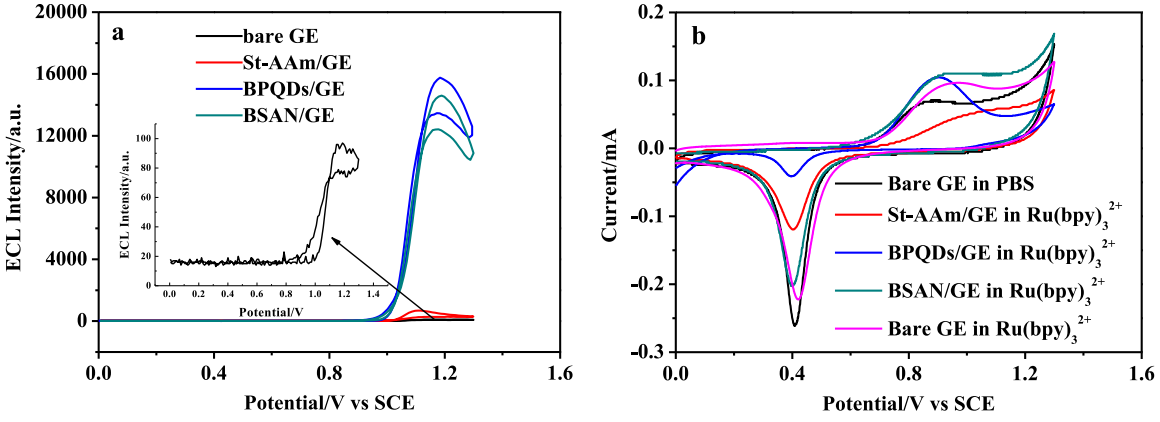

Fig. 3. ECL (a) and electrochemical (b) behaviors of different gold electrodes in 0.1 mol L^{-1} PBS containing 0.1 mM $Ru(bpy)_3^{2+}$. scan rate, 100 mV s^{-1}; pH, 7.4. The inset is the enlarged ECL curve of bare GE in $Ru(bpy)_3^{2+}$ solution.

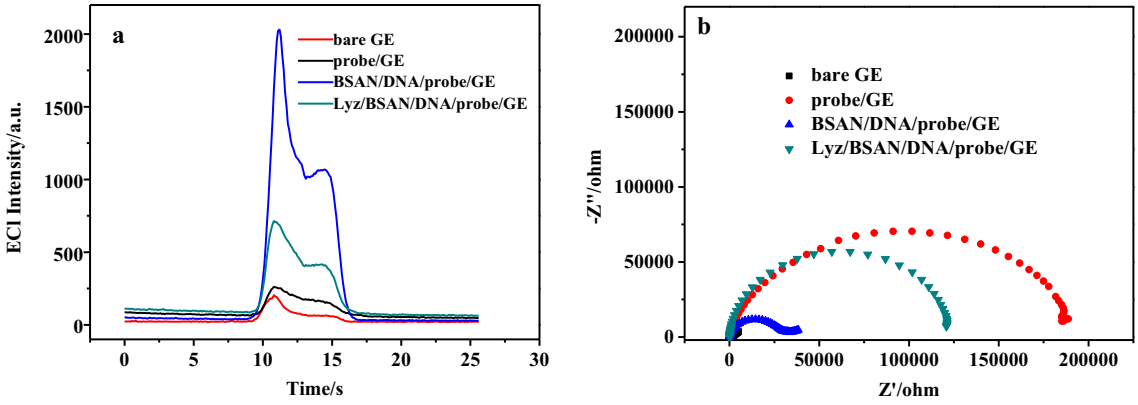

Fig. 4. (a) ECL profiles of different processes of the fabrication of aptasensor, lysozyme, 40 pg mL^{-1}, PBS, 0.1 mol L^{-1}, pH, 7.4; scan rate, 100 mV s^{-1}. (b) Nyquist diagram of electrochemical impedance spectra recorded from 0.01 to 10^5 Hz for $[Fe(CN)_6]^{3-/4-}$ (10 mM, 1:1) in 0.1 mol L^{-1} pH 7.4 PBS containing 0.1 mol L^{-1} KCl.

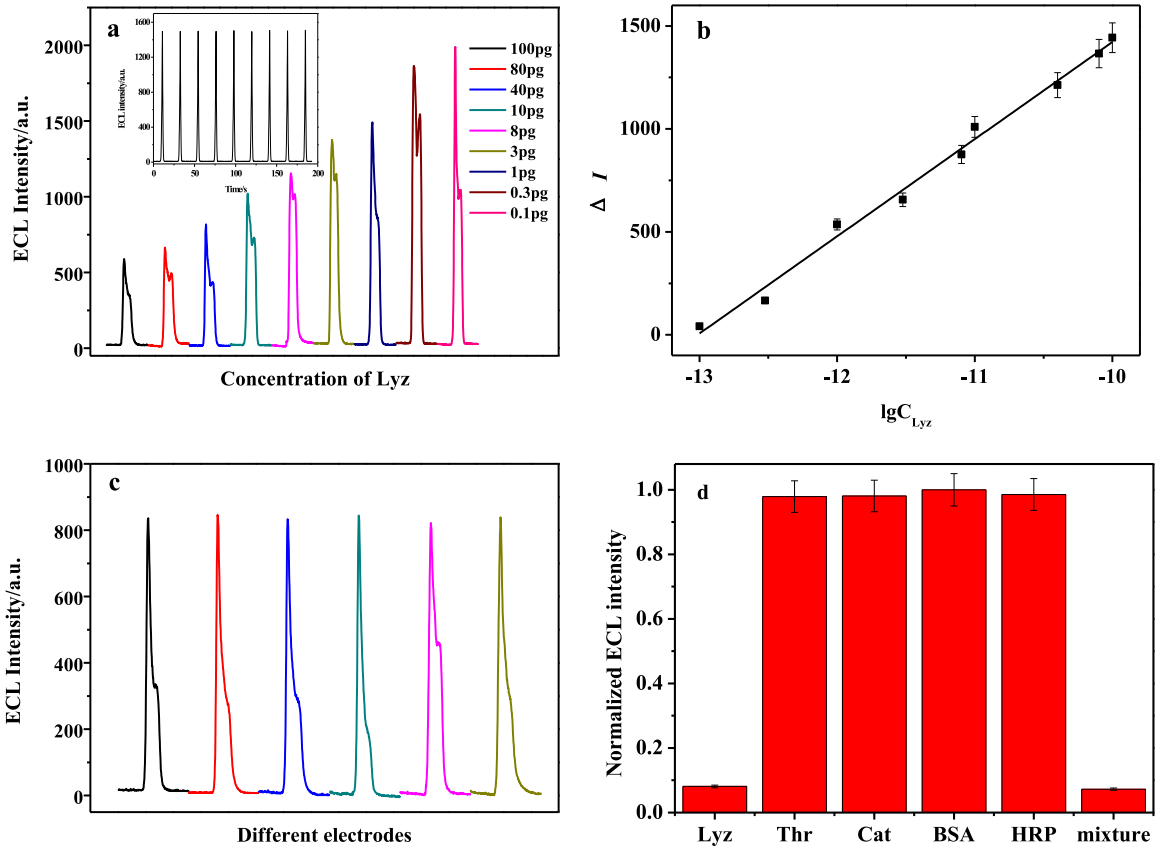

Fig. 5. (a) ECL signals of the aptasensor incubated with different concentration of Lyz (from 0.1 to 100 pg mL^{-1}). The inset is the stability of the aptasensor in 1 pg mL^{-1} Lyz under 9-cycles continuous potential scan. (b) Logarithmic calibration curve between ECL intensity decrement and Lyz concentration. (c) Reproducibility of six sensors for the determination of 10 pg mL^{-1} Lyz. (d) Selectivity of the aptasensor to Lyz comparing with possible interfering proteins. BSA, HRP, Lyz, Thr, Cat at 10 pg mL^{-1}, respectively.

diffusion of the redox probe through the electrode surface. It can be found from Fig. 4b that the bare GE exhibits nearly straight line in the whole frequency range, revealing the facile electron transfer through the electrode surface. When the aptamer is modified on the GE, the R_{ct} increases greatly due to the electrostatic repulsion between negatively charged DNA aptamer backbone and $[Fe(CN)_6]^{3-/4-}$ probe. When BSAN/DNA is hybridized with the aptamer, the R_{ct} decreases apparently due to the good conductivity of BPQDs. When BSAN/DNA is replaced by Lyz, the R_{ct} increases again. The EIS results support the successful stepwise fabrication of the proposed ECL aptasensor.

3.4. Analytical performance of ECL aptasensor

Generally, the performance of biosensor including lifetime, linear range, sensitivity, selectivity, stability, and susceptibility to interfering agents, and so on. In order to evaluate the sensing performances of proposed aptasensor, the above parameters were investigated. The linear range for Lyz was tested by measuring the ECL intensities after the aptasensor was incubated in different concentration of Lyz. It can be found from Fig. 5a that the ECL intensity decreases gradually with the increase of Lyz concentrations from 0.1 to 100 pg mL^{-1}. The inset of Fig. 5a is the 9-cycles continuous determination of 1 pg mL^{-1} Lyz using the proposed aptasensor. It can be seen that the aptasensor exhibits

satisfactory stability with a relative standard deviation (RSD) of 0.56%. Fig. 5b shows a good linear relationship between ECL intensity decrement $\Delta I = I_0 - I$ (where I_0 and I are the ECL intensity without and with Lyz, respectively) and logarithm of Lyz concentration. The linear regression equation is determined as $\Delta I = 6140 + 451.1 \log C$ with the correlation coefficient of 0.991. The detection limit of the aptasensor is calculated as 2.9×10^{-14} g mL^{-1} (3σ, n = 6). The reproducibility of the proposed aptasensor for Lyz is evaluated from the responses to 10 pg mL^{-1} Lyz at six biosensors which were fabricated under the same condition. These sensors exhibit the similar ECL responses and the relative standard deviation is 1.2%. Therefore, the reproducibility of the aptasensors for the detection of Lyz is acceptable. The long-term stability of the aptasensor was tested by measuring ECL every day, and it was stored in refrigerator when it was not used. The ECL signal retains 90% of the original response after three weeks, indicating good long-term stability of the aptasensor.

The specificity of the proposed aptasensor for Lyz was evaluated as shown in Fig. 5d. In the experiment, 10 pg mL^{-1} of thrombin (Thr), bovine serum albumin (BSA), horse radish peroxidase (HRP), catalase (Cat) and Lyz, were tested under the same process. It is observed that only Lyz sample can significantly inhibit ECL emission. Meanwhile, the mixture between Lyz and these proteins shows the similar inhibiting effect on ECL emission as that of pure Lyz. These results indicate the high specificity of the proposed aptasensor to Lyz. The comparison of various techniques for the detection of Lyz is listed in Table S1. Although the detection limit of the present aptasensor is slightly higher than our previous work, it still exhibits advantage over other work. Most importantly, the first report on biosensing application of BP nanomaterials is attractive in the fabrication of ECL biosensor with 2D materials. The potential applicability of the aptasensor in real sample was investigated by detecting Lyz in human serum samples which were obtained from local hospital. The serum 1:5 diluted with PBS was spiked with Lyz at different concentrations, and the standard addition method was used to detect Lyz. The results listed in Table S2 show the acceptable relative standard deviation and good recoveries, implying that the proposed aptasensor is promising applicable in real samples.

4. Conclusions

The lack of functional group on BPQDs limit its application in the fabrication of biosensor. The present work revealed that styrene-acrylamide copolymer can be used to encapsulate BPQDs to form functional nanospheres, which can act as coreactant to react with $Ru(bpy)_3^{2+}$ to generate strong anodic ECL singal. Amino group of polymer film endow BPQDs the ability to contact with DNA. As a result, an aptasensor for the detection of lysozyme is fabricated. Under the optimal condition, lysozyme can be sensitively detected in the range of 1.0×10^{-13}-1.0×10^{-10} g mL^{-1}, with a detection limit of 2.9×10^{-14} g mL^{-1} (3σ). The aptasensor exhibits good long-term stability, satisfied repeatability, reproducibility, and excellent specificity. Although the detection limit of the aptasensor is slightly higher than the previous work, it is still attractive for the biosensing application of BP nanomaterials.

Acknowledgements

This work is financially supported by National Natural Science Foundation of China (Nos. 21575002, 61671019).

Appendix A. Supporting information

Supplementary data associated with this article can be found in the online version at doi:10.1016/j.talanta.2019.02.099.

References

[1] M.R. Ganjali, H. Beitollahi, R. Zaimbashi, S. Tajik, M. Rezapour, B. Larijani, Int. J. Electrochem. Sci. 13 (2018) 2519–2529.
[2] H. Beitollahi, Z. Dourandish, S. Tajik, M.R. Ganjali, P. Norouzi, F. Faridbod, J. Rare Earths 36 (2018) 750–757.
[3] M.R. Ganjali, Z. Dourandish, H. Beitollahi, S. Tajik, L. Hajiaghababaei, B. Larijani, Int. J. Electrochem. Sci. 13 (2018) 2448–2461.
[4] M.H. Beitollahi, S. Tajik, M.R. Aflatoonian, A. Makarem, Anal. Bioanal. Electrochem. 10 (2018) 1399–1413.
[5] H. Beitollahi, M. Safaei, M.R. Shishehbore, S. Tajik, J. Electrochem. Sci. Eng. 9 (2019) 45–53.
[6] H. Beitollahi, M. Safaei, S. Tajik, J. Electrochem. Sci. Eng. 9 (2019) 27–43.
[7] S. Tajik, H. Beitollahi, P. Biparva, J. Serb. Chem. Soc. 83 (2018) 863–874.
[8] S. Tajik, H. Beitollahi, Anal. Bioanal. Chem. Res. 6 (2019) 171–182.
[9] M. Pumera, A.H. Loo, Trend Anal. Chem. 61 (2014) 49–53.
[10] A. Martin, A. Escarpa, Trend Anal. Chem. 56 (2014) 13–26.
[11] L.K. Li, Y.J. Yu, G.J. Ye, Q.Q. Ge, X.D. Ou, H. Wu, D.L. Feng, X.H. Chen, Y.B. Zhang, Nat. Nanotechnol. 9 (2014) 372–377.
[12] H.O.H. Churchill, P. Jarillo-Herrero, Nat. Nanotechnol. 9 (2014) 330–331.
[13] F.N. Xia, H. Wang, Y.C. Jia, Nat. Commun. 5 (2014) 4458.
[14] M. Buscema, D.J. Groenendijk, S.I. Blanter, G.A. Steele, H.S.J. van der Zant, A. Castellanos-Gomez, Nano Lett. 14 (2014) 3347–3352.
[15] A. Favron, E. Gaufres, F. Fossard, A.L. Phaneuf-L'Heureux, N.Y.W. Tang, P.L. Levesque, A. Loiseau, R. Leonelli, S. Francoeur, R. Martel, Nat. Mater. 14 (2015) 826–832.
[16] H.T. Yuan, X.G. Liu, F. Afshinmanesh, W. Li, G. Xu, J. Sun, B. Lian, A.G. Curto, G.J. Ye, Y. Hikita, Z.X. Shen, S.C. Zhang, X.H. Chen, M. Brongersma, H.Y. Hwang, Y. Cui, Nat. Nanotechnol. 10 (2015) 707–713.
[17] Z.B. Yang, J.H. Hao, S.G. Yuan, S.H. Lin, H.M. Yau, J.Y. Dai, S.P. Lau, Adv. Mater. 27 (2015) 3748–3754.
[18] K.A. Ritter, J.W. Lyding, Nat. Mater. 8 (2009) 235–242.
[19] S.N. Baker, G.A. Baker, Angew. Chem. 122 (2010) (6876-6796).
[20] J.O. Island, G.A. Steele, H.S.J. van der Zant, A. Castellanos-Gomez, 2D Mater. 2 (2015) 011002.
[21] X. Zhao, Y. Liu, H. Hui, J. Med. Coll. PLA 12 (1997) 62–65.
[22] G.P. Wang, E.Q. Song, H.Y. Xie, Z.L. Zhang, Z.Q. Tian, C. Zuo, D.W. Pang, D.C. Wu, Y.B. Shi, Chem. Commun. 41 (2005) 4276–4278.
[23] M. Xie, J. Hu, Y.M. Long, Z.L. Zhang, H.Y. Xie, D.W. Pang, Biosens. Bioelectron. 24 (2009) 1311–1317.
[24] E.Q. Song, G.P. Wang, H.Y. Xie, Z.L. Zhang, J. Hu, J. Peng, D.C. Wu, Y.B. Shi, D.W. Pang, Clin. Chem. 53 (2007) 2177–2185.
[25] J. Hu, M. Xie, C.Y. Wen, Z.L. Zhang, H.Y. Xie, A.A. Liu, Y.Y. Chen, S.M. Zhou, D.W. Pang, Biomaterials 32 (2011) 1177–1184.
[26] E.Q. Song, J. Hu, C.Y. Wen, Z.Q. Tian, X. Yu, Z.L. Zhang, Y.B. Shi, D.W. Pang, ACS Nano 5 (2011) 761–770.
[27] C.Y. Wen, J. Hu, Z.L. Zhang, Z.Q. Tian, G.P. Ou, Y.L. Liao, Y. Li, M. Xie, Z.Y. Sun, D.W. Pang, Anal. Chem. 85 (2013) 1223–1230.
[28] W.J. Miao, A.J. Bard, Anal. Chem. 75 (2003) 5825–5834.
[29] E.G. Hvastkovs, M. So, S. Krishnan, B. Bajrami, M. Tarun, I. Jansson, J.B. Schenkman, J.F. Rusling, Anal. Chem. 79 (2007) 1897–1906.
[30] F. Deiss, C.N. LaFratta, M. Symer, T.M. Blicharz, N. Sojic, D.R. Walt, J. Am. Chem. Soc. 131 (2009) 6088–6089.
[31] N. Egashira, S.I. Moria, E. Hifumi, Y. Mitoma, T. Uda, Anal. Chem. 80 (2008) 4020–4025.
[32] J. Zhang, H.L. Qi, Y. Li, J. Yang, Q. Gao, C.X. Zhang, Anal. Chem. 80 (2008) 2888–2894.
[33] Z.J. Lin, X.M. Chen, T.T. Jia, X.D. Wang, Z.X. Xie, M. Oyama, X. Chen, Anal. Chem. 81 (2009) 830–833.
[34] I.S. Shin, S.W. Bae, H. Kim, J.I. Hong, Anal. Chem. 82 (2010) 8259–8265.
[35] Y.W. Chi, Y.Q. Dong, G.N. Chen, Anal. Chem. 79 (2007) 4521–4528.
[36] M. Zorzi, P. Pastore, F. Magno, Anal. Chem. 72 (2000) 4934–4939.
[37] H.N. Choi, S.H. Cho, W.Y. Lee, Anal. Chem. 75 (2003) 4250–4256.
[38] K.F. Chow, F. Mavré, J.A. Crooks, B.Y. Chang, R.M. Crooks, J. Am. Chem. Soc. 131 (2009) 8364–8365.
[39] Y.P. Dong, T.T. Gao, Y. Zhou, L.P. Jiang, J.J. Zhu, Sci. Rep. 5 (2015) 15392.
[40] L. Zhang, K.J. Tian, Y.P. Dong, H.C. Ding, C.M. Wang, Analyst 143 (2018) 304–310.
[41] X.R. Zhang, Y.Q. Zhao, H.R. Zhou, B. Qu, Biosens. Bioelectron. 26 (2011) 2737–2741.
[42] Z.H. Zhang, S. Zhang, L.H. He, D.L. Peng, F.F. Yan, M.H. Wang, J.H. Zhao, H.Z. Zhang, S.M. Fang, Biosens. Bioelectron. 74 (2015) 384–390.
[43] A.K.H. Cheng, B.X. Ge, H.Z. Yu, Anal. Chem. 79 (2007) 5158–5164.
[44] D. Tang, D.L. Liao, Q.K. Zhu, F.Y. Wang, H.P. Jiao, Y.J. Zhang, C. Yu, Chem. Commun. 47 (2011) 5485–5487.
[45] X. Zhang, H.M. Xie, Z.D. Liu, C.L. Tan, Z.M. Luo, H. Li, J.D. Lin, L.Q. Sun, W. Chen, Z.C. Xu, L.H. Xie, W. Huang, H. Zhang, Angew. Chem. 127 (2015) 3724–3728.
[46] Z.B. Sun, H.H. Xie, S.Y. Tang, X.F. Yu, Z.N. Guo, J.D. Shao, H. Zhang, H. Huang, H.Y. Wang, P.K. Chu, Angew. Chem. 127 (2015) 11688–11692.
[47] Y.P. Dong, H. Cui, C.M. Wang, J. Phys. Chem. B 110 (2006) 18408–19414.